Science of the Total Environment 1030 (2026) 181774

Contents lists available at ScienceDirect

Science of the Total Environment

journal homepage: www.elsevier.com/locate/scitotenv

Revised estimates of forest carbon sequestration reveal the true sink capacity of Japanese forests

Tomo'omi Kumagai [a,b,*], Ryo Nakahata [a,c], Toshiaki Kameyama [a], Tomohiro Egusa [d]

[a] Graduate School of Agricultural and Life Sciences, The University of Tokyo, 1-1-1 Yayoi, Bunkyo-ku, Tokyo 113-8657, Japan
[b] Water Resources Research Center, University of Hawai'i at Mānoa, 2540 Dole St., Holmes Hall 283, Honolulu, HI 96822, USA
[c] Center for Tree Science, The Morton Arboretum, 4100 Illinois Route 53, Lisle, IL 60532, USA
[d] Faculty of Agriculture, Shizuoka University, 836 Ohya, Suruga-ku, Shizuoka 422-8529, Japan

HIGHLIGHTS

- Direct forest measurements show Japan's carbon uptake is double earlier estimates.
- Annual forest carbon sequestration in Japan reached 46.2 TgC yr^{-1} in recent surveys.
- *Cryptomeria japonica* accounts for 43.1% of Japan's total annual carbon sequestration.
- Forest type and stem volume are identified as the main drivers of productivity.
- High-accuracy inventory data are crucial for Japan's carbon neutrality planning.

GRAPHICAL ABSTRACT

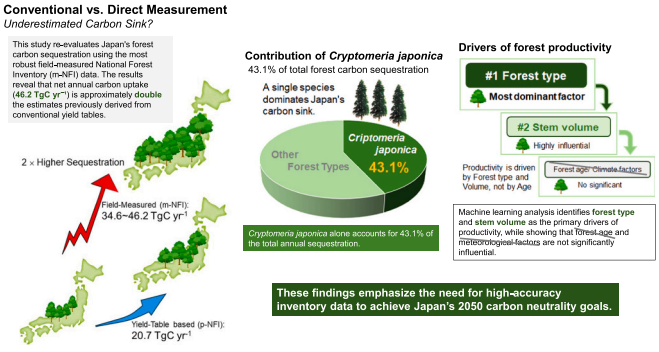

ARTICLE INFO

Keywords:
Carbon stock
Forest productivity
Net ecosystem productivity
Carbon neutral
Tree census
Forestry practice
Shapley additive explanation (SHAP)

ABSTRACT

An accurate estimate of total forest carbon sequestration is crucial to develop effective strategies for wood production and reduce CO_2 emissions. Japan's National Forest Inventory (NFI) collects data on stand stem volumes in forests across Japan. The inventory based on direct field measurements of individual tree sizes (m-NFI) is regarded as the most accurate and robust. Thus, the difference in m-NFI-derived carbon stock estimates between consecutive inventory surveys is considered the most reliable estimate of forest carbon uptake rates. Here, we show that net annual carbon uptake estimated from the m-NFI conducted in the periods 2009–2013 (third NFI) and 2014–2018 (fourth NFI) is 34.6 and 46.2 TgC yr^{-1} for forests managed under the governmental management plan (m-NFI_1) and all forest categories (m-NFI_2), respectively. These are approximately double the estimates from the NFI based on the predictions from yield tables (p-NFI), which Japanese national and local forestry agencies have conventionally used. Notably, *Cryptomeria japonica*, the most important plantation tree species for timber production in Japan, has the highest area-based carbon uptake rate among the studied forest types and, despite being a single tree species, accounts for 43.1% of Japan's total annual forest carbon sequestration. Further investigation using a machine-learning algorithm revealed that the primary factor controlling total forest productivity is the forest type, followed by stem volume. Forest age and meteorological drivers are not significantly

* Corresponding author at: Graduate School of Agricultural and Life Sciences, The University of Tokyo, 1-1-1 Yayoi, Bunkyo-ku, Tokyo 113-8657, Japan.
E-mail address: tomoomikumagai@gmail.com (T. Kumagai).

https://doi.org/10.1016/j.scitotenv.2026.181774
Received 22 January 2026; Received in revised form 2 April 2026; Accepted 2 April 2026
Available online 14 April 2026

influential. We emphasize the importance of accounting for high forest productivity in planning for future forestry and carbon neutrality in Japan.

1. Introduction

Forests are the dominant component of the terrestrial carbon (C) sink, significantly affecting the atmospheric CO_2 concentration and global warming (e.g., Booth et al., 2012). Therefore, knowledge of the sequestration of atmospheric C in regional-scale forests is vital. Forest inventory based on biometric methods, i.e., tree-to-tree measurements of size, species, and biomass, is considered the most accurate analysis method for assessing forest dynamics, e.g., growth, harvest, and mortality, and for estimating forest C sinks at the regional and national scales (see Pan et al., 2024). Although forest C sinks have been evaluated using eddy-covariance measurements (e.g., Hata et al., 2023; Kondo et al., 2017; Takamura et al., 2023), remote sensing (e.g., Dubayah et al., 2022; Hilker et al., 2008; Li et al., 2024; Mermoz et al., 2015; Pei et al., 2022), and terrestrial ecosystem modeling (e.g., Ito, 2008; Sasai et al., 2011), a large-scale forest inventory remains the most reliable tool for validation of the results.

A national forest inventory (NFI) is a nationwide forest survey that historically aims to estimate timber productivity. An NFI generally includes information on tree species composition and stand- or individual-tree-scale stem volume in targeted forests. Many studies have used NFI data to clarify forest C stocks and net C uptake from the past to the present (Birdsey et al., 1993; Ciais et al., 2008; Fang et al., 2001; Kauppi et al., 2010; Kauppi et al., 1992; Pan et al., 2024; Pan et al., 2011) and to predict their future changes with forest growth models (Eggers et al., 2008; Hu et al., 2015; Wear and Coulston, 2015).

In Japan, two types of NFI have been performed: one based on predictions from yield tables (p-NFI) and the other based on direct field measurements of individual tree sizes (m-NFI). The current p-NFI was initiated in 1975, with yield tables constructed using actual observation data from around 1970, whereas the m-NFI surveys were conducted in 1961, 1966, and, following a long gap, in 1999, employing revised sampling methods (see Egusa et al., 2020). The m-NFI surveys in 1999–2003 (first NFI) and 2004–2008 (second NFI) were found to underestimate stem volume. To resolve this, the m-NFI in 2009–2013 (third NFI) incorporated expert accuracy checks and technical training for surveyors. These measures ensured that the third NFI achieved the highest reliability among the Japanese NFIs (see Kitahara et al., 2009).

Our previous work (Egusa et al., 2020) demonstrated that the national total forest C uptake estimated using p-NFI (19.9 TgC yr^{-1}), which Japanese public forestry agencies have believed to be authentic, was greatly underestimated compared with the estimate from the m-NFI (48.5 TgC yr^{-1}), suggesting that the underestimation of forest biomass predominantly reflected the outdated yield tables. This work estimated forest C sequestration across Japan by calculating the difference in m-NFI-derived C stock between 1966 and 2011, the midpoint of the third NFI period. The potential error in the carbon stock estimation in the first and second NFIs, combined with the relatively short interval between those surveys, would compromise accurate estimation of the annual net forest C uptake across Japan. Thus, despite the significantly different survey protocols between the 1966 m-NFI and the third NFI, Egusa et al. (2020) were required to account for the long-term difference in C stocks between those datasets for the annual estimation of forest C sequestration.

Ideally, forest C uptake should be estimated as the difference in elaborated C stocks between surveys, with an interval of approximately 5 years to consider the temporal variation in the forest C sink/source and its response to a changing climate. Hence, our primary goal was to provide an accurate estimate of forest C sequestration across Japan. To achieve this, we utilized the third NFI data and the latest m-NFI data from 2014 to 2018 (fourth NFI), enabling the most reliable calculation of differences in C stock estimates between these two inventories. In addition, we examined the spatial variation in forest productivity across Japan and the factors controlling the potential productivity.

2. Materials and methods

2.1. Data

In this study, we utilized the C stocks derived from the p-NFI data for 2002, 2007, and 2012, as well as the m-NFI data from the third and fourth NFIs. The forests managed under a long-term governmental management plan, as defined in the Japanese Forest Acts (JFA), were surveyed for the p-NFI. All forest categories, including the JFA-governed forests, forests without a governmental management plan, and cut-over and potential forests, were included in the m-NFI. For comparison between the previous estimates of forest C sequestration and the present estimate, the m-NFI data were categorized into two types: data from JFA forests only (m-NFI_1) and all forest categories (m-NFI_2). Although a detailed explanation is provided elsewhere (Egusa et al., 2020), a description of p-NFI and m-NFI is provided below for completeness.

2.1.1. National forest inventory based on yield table predictions: p-NFI

The yield tables used in the p-NFI are empirical relationships between stand-scale stem volume, age class (ranked from 1 at 5-year intervals), and the land productivity index for each important tree species. The forests are categorized into two types for p-NFI: plantations and natural forests. Data for plantations comprise stem volume and forest area, which are further categorized into 10 forest types, 47 prefectures, and 19 age classes. Data for natural forests comprise only stem volume categorized into 11 forest types and 47 prefectures. Notably, no information is provided on the forest area for each natural forest type.

The yield tables used for the 2002, 2007, and 2012 p-NFI data were constructed based on actual measurements recorded around 1970. The yield tables for forests in Japan differ depending on the type of forest ownership. The yield tables generated by the national government have been used for national forests, accounting for approximately 30% of the total forest area. Each of the 47 prefectural governments has created its own yield tables for local-government-owned and private forests, accounting for approximately 70% of the forest area. Most yield tables are unpublished and even the national forestry agency does not know all the information on their yield tables. More specifically, although the land productivity index is critical for estimating the stem volume in a given stand, no standard procedure is established for determining this index for many target forest stands. To our knowledge, no national and local forestry agencies are able to revise the land productivity index, which can be affected by various environmental changes and is a significant source of error in stem volume estimation.

The Japan Forestry Agency has aggregated the data submitted by administrators for national and prefectural forests and published estimates of the stem volume, together with additional relevant information (https://www.rinya.maff.go.jp/j/keikaku/genkyou/index1.html).

2.1.2. National forest inventory based on direct field measurements: m-NFI

In one campaign of the current m-NFI survey, direct field biometric measurements were recorded over 5 years. The m-NFI is designed with a 4 km interval grid covering approximately 23,000 points across Japan. Measurements were performed at the given plots that include forests. The third and fourth NFIs were conducted in 2009–2013 and 2014–2018, respectively; the data are accessible from the National Forest Inventory of Japan website (http://forestbio.jp/index.html). From the initial grid, the number of plots categorized as “forests” for the

third and fourth NFIs was initially 16,139 and 16,078, respectively, but was reduced to 14,800 and 14,087, owing to accessibility issues. Standing tree plots, i.e., the target plots, were selected by eliminating "potential forest" plots, such as bamboo, cut-over land, and unidentified forest plots, resulting in the retention of 13,061 and 12,485 plots for the third and fourth NFIs, respectively (see Table 1).

Using aerial photographs, satellite imagery, and field surveys, Japan's total forest areas for the third and fourth NFIs are estimated to be 25.86 and 25.76 Mha, respectively (https://www.rinya.maff.go.jp/j/keikaku/tayouseichousa/tikuseki.html). These estimations include the potential forest areas, which are 1.92 and 2.64 Mha for the third and fourth NFIs, respectively. Deducting the potential forest area from the total forest area, the areas for m-NFI_1 in the third and fourth NFIs are estimated to be 23.9 and 23.1 Mha, respectively (see Table 1). The m-NFI_2 area was estimated by adding 50% of the potential forest area to the m-NFI_1 area. This 0.5 ratio was derived from the fourth NFI data, in which unidentified forest plots accounted for 53% of the total area of bamboo, cut-over land, and unidentified plots. The resulting areas for the third and fourth NFIs were 24.9 and 24.4 Mha, respectively.

Each plot comprises triple concentric circles with areas of 0.01, 0.04, and 0.1 ha. In the largest (0.1 ha), intermediate (0.04 ha), and smallest (0.01 ha) circular areas, the diameter at breast height (DBH) of trees with DBH greater than 18, 5, and 1 cm, respectively, is measured. Tree height is measured for each of the selected 20 trees in the plot, and tree heights of the remaining trees are estimated using the DBH–tree height relationships (the Näslund function) derived from the measurements for the 20 trees. Stem volume of a single tree is given by the empirical function of DBH and tree height (Hosoda et al., 2010) for each tree species and its growing region, as proposed by the Japan Forestry Agency (1970a, 1970b).

In this study, we used publicly available data consisting of plot-level aggregated information rather than individual tree-scale data. The data comprised stem volume per hectare (V_s; m^3 ha^{-1}), dominant species, forest age, and the history of natural disturbances and forestry practices for each plot. The annual mean differences in V_s between the practical measurements and the validation surveys were 4%–8%, likely indicating underestimation, for the third and fourth NFIs (Japan Forestry Agency, 2015, 2019). The dominant tree species is the species with the largest total cross-sectional area at breast height in the plot, which in turn determines the forest type of the plot. Table 1 presents a list of forest types used in this study, the number of observation plots, and the area based on m-NFI_1 for the third and fourth NFIs.

2.2. Carbon stock estimation

Forest stand-scale C density (C_d; MgC ha^{-1}) was calculated in accordance with Fang et al. (2005):

$$C_d = V_s \times BEF \times 0.5 \quad (1)$$

in which

$$BEF = \min\left(a + \frac{b}{V_s},\ 1.5\right), \quad (2)$$

where 0.5 is the C content ratio (MgC Mg^{-1}) and a (Mg m^{-3}) and b (Mg ha^{-1}) are empirical parameters obtained for a given forest type. BEF is the biomass expansion factor (Mg m^{-3}), which enables the conversion of V_s to stand-scale C_d, including branches, leaves, and roots. The term "min $(\cdot,\cdot)$" represents the minimum of the two factors and is used to avoid unrealistically large values of BEF in cases where the V_s value is minimal. In this study, the upper limit for the BEF was set at 1.5. This threshold was derived from the empirical data for *Cr. japonica* in Fang et al. (2005), which indicates that BEF values can reach approximately 1.5 when extrapolated to minimal V_s levels. We adopted 1.5 as a conservative "cap" to prevent the mathematical overestimation of BEF at very low V_s, while ensuring that the biomass of young stands is not underestimated.

Although we previously reported the method for estimating p-NFI-derived C stocks for 2002, 2007, and 2012 (Egusa et al., 2020), we provide the following summary for completeness. We calculated V_s in plantations by dividing the p-NFI-derived stem volume by the forest area for each factor, i.e., prefecture, forest type, and age class. The C_d was obtained using Eq. (1) with the BEF calculation as described in Eq. (2). The C stocks of plantations were estimated by multiplying the C_d by the forest area for each factor and summing the products. No information on the forest area in the p-NFI natural forest category is available; therefore, we estimated the C stock in natural forests without using V_s. We first derived the BEF values for each prefecture and forest type from the plantations and used these in place of those for natural forests. Then, the C stock in natural forests was estimated by multiplying the BEF by the total stem volume for each prefecture and forest type, and then summing the products. The sum of the C stocks in plantations and natural forests determined the total forest C stock across Japan.

To estimate the m-NFI-derived C stock, we calculated C_d with Eq. (1) in each plot using the BEF value derived with Eq. (2), which was determined for the dominant tree species in that plot. We then obtained the plot-averaged C_d for each of the 12 forest types in Table 1. The C stock for each forest type was calculated by multiplying the forest type's average C_d and forest type area, and the sum represented the total forest C stock.

2.3. Net ecosystem productivity estimation and the controlling factors

Given the stable soil C storage during the m-NFI campaign, using the C_d for each remeasured plot between the third and fourth NFI cycles calculated with Eq. (1), the forest stand-scale C uptake (C_{UP}; MgC ha^{-1} yr^{-1}) was calculated as:

$$C_{UP} = \frac{C_{d_{4th}} - C_{d_{3rd}}}{\Delta t}, \quad (3)$$

where the subscripts 4th and 3rd denote the values for the fourth and third NFIs, respectively, and Δt is the interval between the third and fourth NFIs, which is assumed to be 5 years as a plot-averaged value. Here, we estimated the net ecosystem productivity (NEP) by excluding data points affected by natural disturbances and forestry practices from the C_{UP}. Specifically, to distinguish these impacts, C_{UP} values influenced by biomass loss due to natural disturbances were defined as NEP_Dist, while those reflecting harvested volume or biomass from forestry practices were categorized as NEP_For.

A spatial distribution of the annual-averaged meteorological drivers during the m-NFI campaign period (2008–2018) across Japan was constructed using a daily grid (1 km × 1 km) meteorological dataset obtained from the Agro-Meteorological Grid Square Data, National

Table 1
List of forest types used in this study, number of observation plots, and area based on m-NFI_1 for the third and fourth NFIs.

Forest type	Number of observation plots (Area; Mha)	
	Third NFI	Fourth NFI
Cryptomeria japonica	2824 (5.18)	2737 (5.07)
Chamaecyparis obtusa	1661 (3.04)	1639 (3.04)
Pinus densiflora	703 (1.29)	621 (1.15)
Larix kaempferi	550 (1.01)	484 (0.90)
Abies and *Picea*	1130 (2.07)	1037 (1.92)
Fagus	717 (1.31)	652 (1.21)
Quercus	1969 (3.61)	1917 (3.55)
Betulaceae	841 (1.54)	815 (1.51)
Coniferous and broad-leaved mixed forests	41 (0.08)	10 (0.02)
Evergreen broad-leaved forests	383 (0.70)	402 (0.74)
Other coniferous forests	255 (0.47)	227 (0.42)
Other broad-leaved forests	1987 (3.64)	1944 (3.60)
Total	13,061 (23.94)	12,485 (23.12)

Agriculture and Food Research Organization, Japan (available at https://amu.rd.naro.go.jp/wiki_open/doku.php?id=start).

We inferred the dependence of NEP in the absence of natural disturbances and forestry practices on forest characteristics and meteorological drivers using Shapley additive explanation (SHAP; Lundberg and Lee, 2017) values, calculated for seven controlling factors, as input for a tree-based machine-learning prediction algorithm (random forests; Breiman, 2001) (cf. Takamura et al., 2023). To ensure model robustness and interpretative transparency, the original dataset (N = 7043) was randomly partitioned into a training and validation set (80%, n = 5634) and an independent test set (20%, n = 1409). The SHAP method, developed in the context of cooperative game theory, assigns a value to each input parameter for a specific model prediction, representing a measure of its contribution to the model's output. We set the forest type, timber volume, and forest age in the third NFI, and annual-averaged meteorological drivers, comprising solar radiation (R_s), precipitation (P), air temperature (T_a), and vapor pressure deficit (VPD), as input parameters.

For the random forest model, hyperparameters were optimized through Bayesian optimization to minimize the five-fold cross-validation MSE exclusively within the training set, using the Statistics and Machine Learning Toolbox (ver. 24.2) in MATLAB. This optimization process involved 5000 iterations to identify the global optimum within the defined search space. To ensure an unbiased selection for categorical features (i.e., forest type), the interaction test was employed for split variable selection. Crucially, all SHAP values used for ecological interpretation were calculated based on the independent test set (n = 1409), which was not involved in the model training or optimization, thereby eliminating any potential overfitting bias. Detailed partitioning and optimization settings are summarized in Appendix Table A1.

3. Results

3.1. Total forest carbon stock and net carbon uptake over Japan

The p-NFI-derived C stocks in 2002, 2007, and 2012 were 1542.2, 1629.6, and 1749.5 TgC, respectively, and the average net C uptake in the period 2002–2012 was 20.7 TgC yr^{-1} (Fig. 1). The mean C stocks and associated 95% confidence intervals (CIs) for m-NFI_1 and m-NFI_2 were 2830.3 ± 24.7 and 2943.8 ± 25.7 TgC, respectively, in the third NFI (n = 13,061) and 3003.1 ± 24.7 and 3174.6 ± 26.1 TgC, respectively, in the fourth NFI (n = 12,485) (see Table 1). These CIs represent the aggregated statistical uncertainty of the total C stocks at the national scale, calculated following the methodology of Egusa et al. (2020). The narrow CIs (relative error < 1%) result from the high statistical power provided by the large-scale integration of plot data across the country. Accordingly, the net C uptake, estimated from the difference between the values in the third and fourth NFIs, was 34.6 and 46.2 TgC yr^{-1} for m-NFI_1 and m-NFI_2, respectively (Fig. 1). The area-based C uptakes for m-NFI_1 and m-NFI_2 were 1.47 and 1.87 MgC ha^{-1} yr^{-1}, respectively.

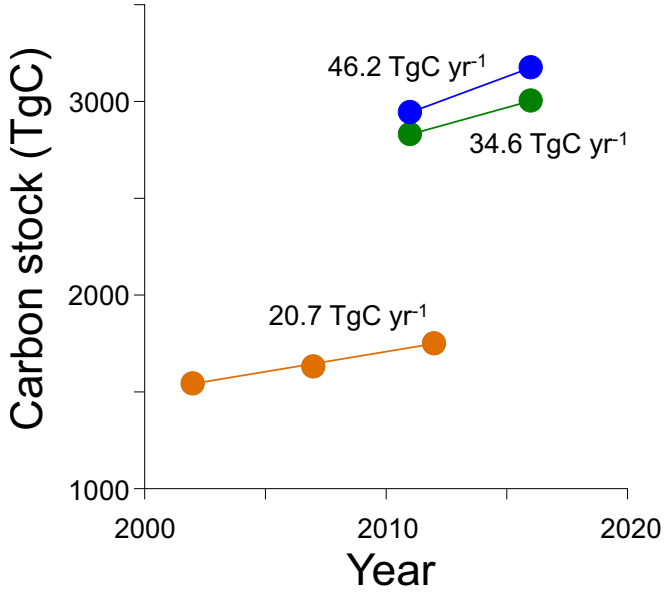

Fig. 1. Temporal changes in total forest C stock in Japan. Estimates based on p-NFI in 2002, 2007, and 2012 (orange solid circles), and m-NFI_1 (green solid circles) and m-NFI_2 (blue solid circles) in 2011 and 2016 are shown. The value beside each circle represents the average net C uptake of each NFI. The 95% confidence interval is too small to be visible.

Based on m-NFI_1 for the major forest types in Japan, which were included in this study (see Table 1), we estimated C stocks and the area-based C stocks (C density) in the third and fourth NFIs, and net C uptake as the difference between the C stocks in the third and fourth NFIs (Fig. 2). *Cryptomeria japonica*, *Chamaecyparis obtusa*, *Fagus*, and *Quercus* had an almost identical C density (approximately 120 MgC ha^{-1}) but differed in area-based forest productivity, which ranged from 3.53 to 1.49 MgC ha^{-1} yr^{-1} for *Cr. japonica* and *Fagus*, respectively (Fig. 2a). *Cryptomeria japonica* and *Quercus* in Japan have the dominant C stocks in their respective forest types because of their dominance in the total forest area (Fig. 2b). Notably, although the C stock of *Cr. japonica* comprised 26.6% of the total forest C stock in Japan, the highest area-based productivity and largest area of this species lead to its highest net C uptake, 14.9 TgC yr^{-1}, in all forest types, accounting for 43.1% of the total forest C uptake.

3.2. Carbon stock and net carbon uptake for the major Japanese forest plantation species

The forest age–area distribution of the major forest plantations, i.e., *Cr. japonica*, *Ch. obtusa*, *P. densiflora*, and *L. kaempferi*, shifted between the third and fourth NFIs consistent with the 5-year interval without changing shape and with little change in each area class (Fig. 3a). This result suggests that harvesting and afforestation were limited in Japanese forest plantations during this NFI campaign period. In contrast, the forest age–C stock distribution shifted between the third and fourth NFIs consistent with the five-year interval but with an increase in C stock in each age class (Fig. 3b). This finding implies that forest C uptake occurred in almost all age classes in the plantations.

The age-class variation in forest plantation C uptake, estimated from the change in C stock between the third and fourth NFIs, was also investigated (Fig. 4). Note that forest age in the third NFI plus 5 years is equivalent to forest age in the fourth NFI. The plantation trees tended to be harvested at an age ranging from 30 to 60 years, with peak harvesting between 35 and 40 years of age, and little harvesting evident at other ages (Fig. 4a). However, despite the larger harvested area at ages 30–60 years, higher C uptakes occurred in the same age classes and decreased at the peak harvest age, because of the larger forest areas (Figs. 3a and 4b). Considering that harvesting lowers the area-based C uptake, we assume that intrinsic forest plantation productivity per forest area is somewhat constant until approximately 75 years of age (Fig. 4c).

3.3. Net ecosystem productivity and its controlling factors across Japan

The spatial variation in forest NEP across Japan was assessed, derived from the difference in forest C stock at each plot between the third and fourth NFIs (Fig. 5). The distribution map of intrinsic forest NEP derived by eliminating the effects of natural disturbances (e.g., windfall and dieoff) and forest practices (e.g., harvest and thinning) shows an apparent tendency for higher forest productivity in southern and western areas of Japan and broadly high productivity over the entire country, including from cool temperate to boreal zones in Hokkaido (Fig. 5a). In addition, we examined the influence on NEP of natural disturbances (NEP_Dist) and forestry practices (NEP_For) across Japan

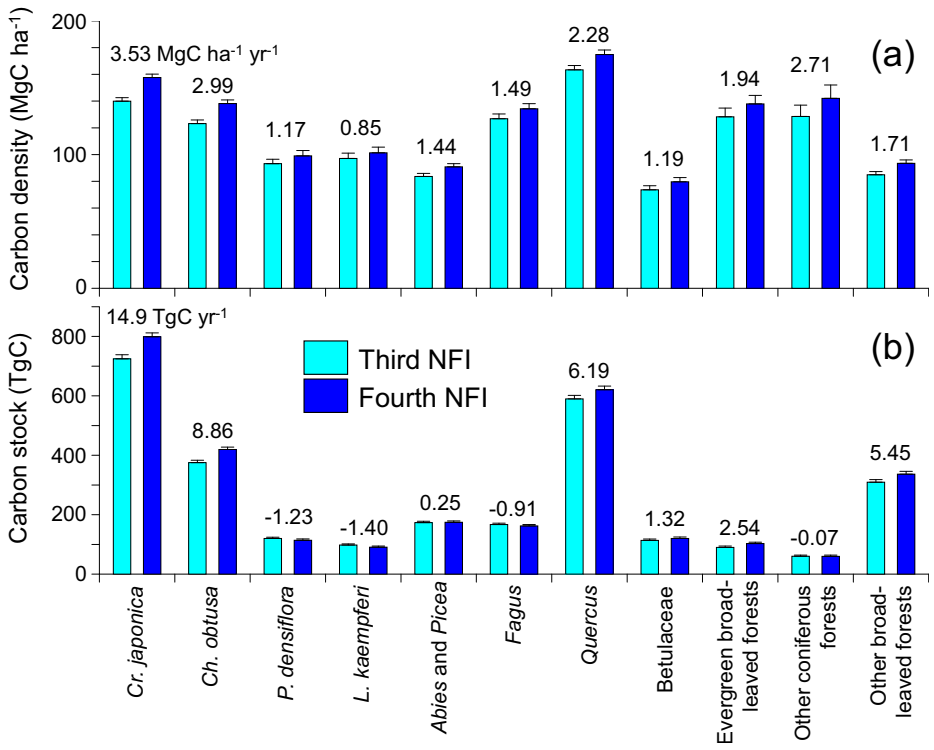

Fig. 2. (a) Carbon density and (b) C stock for each forest type (see Table 1) estimated based on m-NFI_1 using data from the third and fourth NFIs. Error bars represent the upper limits of a 95% confidence interval. The value over each bar represents the average net C uptake for each forest type.

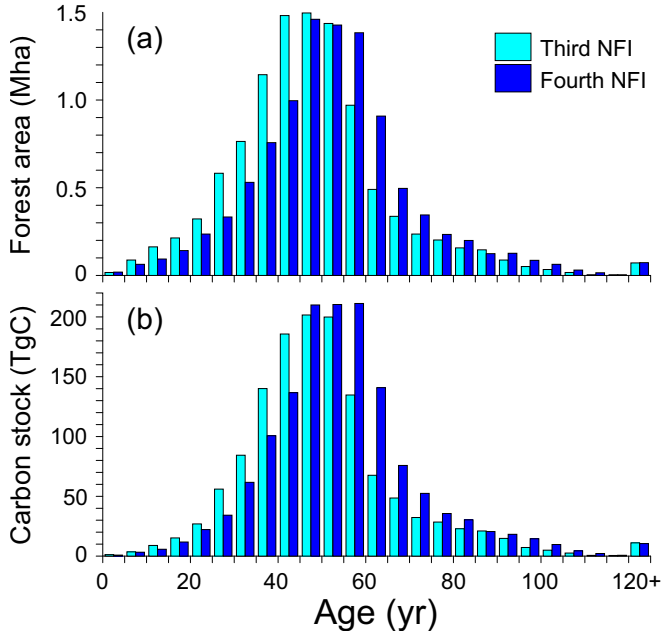

Fig. 3. Temporal changes between the third and fourth NFIs in forest age–area distributions (a) and the forest age–C stock distributions (b) at five-year intervals for the four major forest plantation species in Japan: *Cryptomeria japonica*, *Chamaecyparis obtusa*, *Pinus densiflora*, and *Larix kaempferi*.

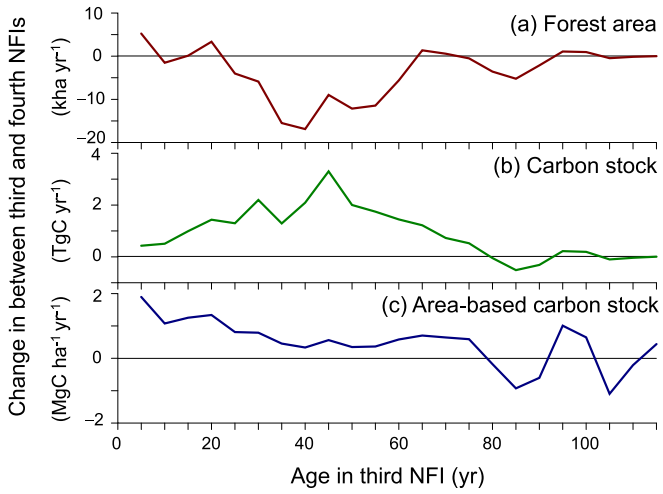

Fig. 4. Changes in forest area (a), C stock (b), and area-based C stock (c) between the third and fourth NFIs as functions of forest age in the third NFI at five-year intervals for the same tree species as in Fig. 3. Note that all values were moving-averaged with a 10-year period to eliminate anomalous fluctuations.

(Fig. 5b). Natural disturbances were uniformly distributed throughout Japan, whereas intense disturbances, caused predominantly by typhoons, tended to be concentrated in Kyushu in southern Japan. Logging was active in the northern part of Honshu and Hokkaido, and intense logging, such as clearance, was detected only in a small area of the country.

We evaluated the contribution of forest characteristics and meteorological drivers to the spatial variation in intrinsic forest NEP (see Fig. 5a). Prior to the factor importance analysis, the predictive performance of the Random Forest (RF) model was validated and compared with a Generalized Linear Model (GLM) assuming a gamma error distribution of the response variable with the log link function. The RF model demonstrated superior predictive performance over the GLM, as detailed in Appendix Table A2, which provides comprehensive validation metrics including R^2, RMSE, and MAE. Based on this validated model, we calculated the mean absolute SHAP value for each controlling

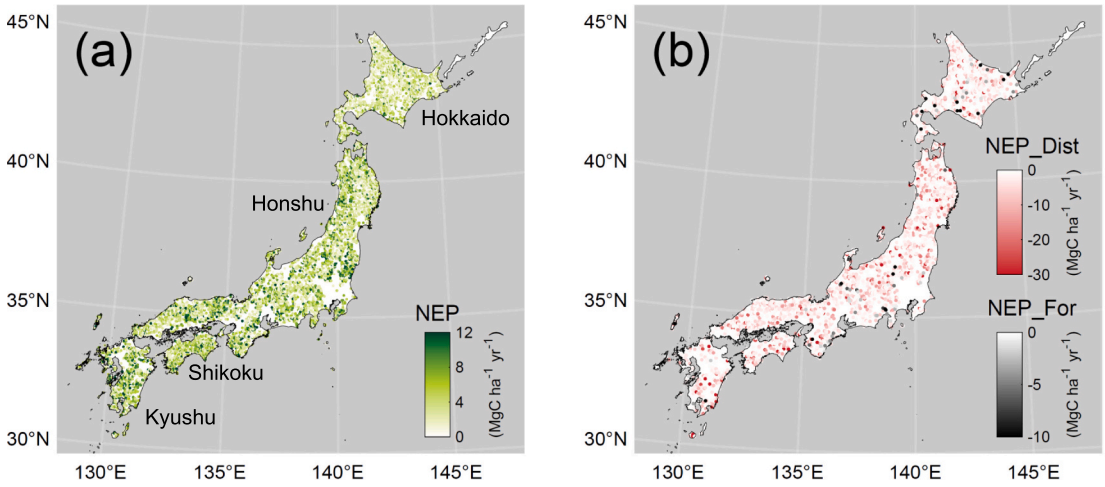

Fig. 5. Spatial distribution of net ecosystem productivity (NEP) without natural disturbances and forestry practices (a) and NEP influenced by natural disturbances (NEP_Dist) and forestry practices (NEP_For) (b) for the main islands of Japan: Hokkaido, Honshu, Shikoku, and Kyushu.

factor (Fig. 6a). Note that SHAP dependency plots used for Fig. 6a are shown in Appendix Fig. A1. Mean absolute SHAP values were almost negligible for most parameters except for forest type and plot-scale timber volume in the third NFI. The most crucial prediction factor was forest type. Thus, we evaluated the contribution of each forest type to NEP variation by calculating the mean SHAP for each controlling factor (Fig. 6b), using the SHAP dependency plot of forest type ID in Fig. A1. In order of decreasing importance, the most important prediction factors were *P. densiflora* and *Abies* and *Picea*, *L. kaempferi* (representing negative contributions), and *Quercus* (representing a positive contribution).

4. Discussion

4.1. Forest carbon stock and uptake

The C stock in 1966 (834.0 TgC) was estimated based solely on the JFA forests; therefore, it is inevitably an underestimate compared with the current m-NFI estimates, which encompass the full range of forest categories. Consequently, the C uptake calculated from the difference between the third NFI stock and the 1966 estimate in our previous work (Egusa et al., 2020) tends to be inherently overestimated when compared with the C uptake derived from the difference between the third and fourth NFIs stocks (i.e., 2943.8 and 3174.6 TgC, respectively; see Fig. 1), where statistical consistency for all forest categories is maintained. The C uptake estimated in the present study (46.2 TgC yr^{-1}) was similar to, but slightly lower than, the estimate by Egusa et al. (2020) (48.5 TgC yr^{-1}).

The Marrakesh Accords stipulate that C removals from properly managed forests can be integrated into national greenhouse gas mitigation plans (UNFCCC, 2002). This principle remains effective under the current Paris Agreement (UNFCCC, 2019). Carbon stock estimates derived from the conventional p-NFI are based on the JFA forests, which correspond to the "managed forests" category defined under the Marrakesh Accords. Consequently, the m-NFI_1 defined in the present study was essential to demonstrate that the conventional p-NFI-based carbon removal estimates, previously reported as national figures, were significantly underestimated. The forest C uptake estimated for m-NFI_1 was 34.6 TgC yr^{-1}, which is substantially higher than the previous

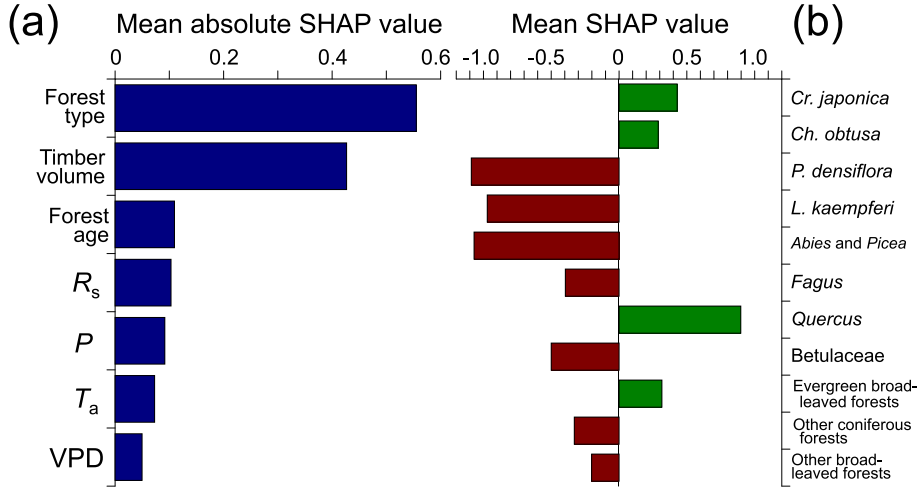

Fig. 6. Contribution of forest characteristics and meteorological drivers (a) and forest types (b) to net ecosystem productivity without natural disturbances and forestry practices. Panels (a) and (b) indicate the mean absolute Shapley additive explanations (SHAP) value for each input feature from forest characteristics and meteorological drivers, and the mean SHAP value for each input feature from forest type categories, respectively. To ensure model robustness and avoid overfitting bias, all SHAP values were calculated exclusively using the independent test set ($n = 1409$). Input features for the tree-based machine-learning model are forest type, timber volume, and forest age in third NFI, and annual-averaged meteorological drivers solar radiation (R_s), precipitation (P), air temperature (T_a), and vapor pressure deficit (VPD) in (a), and 11 forest type categories in (b).

national estimate of 20.7 TgC yr^{-1} (Fig. 1).

In Japan, even when harvested sites are abandoned, woody vegetation establishes relatively quickly, and these areas transition into forests through natural regeneration (Norishige et al., 2025). Consequently, within the m-NFI framework, categories such as cut-over and potential forests are defined as constituent elements of "forest" as they retain a significant level of biomass. Therefore, the actual forest C uptake in Japan corresponds to the value estimated from m-NFI_2 (46.2 TgC yr^{-1}), which is comparable to estimates derived from eddy-covariance measurements, remote sensing, and terrestrial ecosystem modeling. In this study, methods for estimating forest C uptake are characterized by their methodological independence and their roles in validation.

Eddy-covariance measurements (e.g., Takamura et al., 2023) are well established as an independent observational approach. While their validity can be cross-verified against long-term biometric forest inventories, the approach has the unique capability to detect high-frequency environmental responses of forest canopy CO_2 exchange that cannot be captured by biometric surveys. The NEP estimated from eddy-covariance measurements at seven forest sites across Japan ranged from 1.23 to 3.88 MgC ha^{-1} yr^{-1} (Kondo et al., 2017). Our estimates are highly consistent with this independent observational range; the mean m-NFI_2-derived NEP over Japan (1.87 MgC ha^{-1} yr^{-1}) falls well within these bounds, as does the specific range among forest types (from 0.85 MgC ha^{-1} yr^{-1} for *L. kaempferi* to 3.53 MgC ha^{-1} yr^{-1} for *Cr. japonica*; Fig. 2a).

In contrast, methods for NEP estimation from remote-sensing optical data using light-use-efficiency models (see Pei et al., 2022) or terrestrial ecosystem models (e.g., Ito, 2008) are fundamentally dependent on calibration against eddy-covariance data. Therefore, although these models are not considered to be entirely independent estimation methods, terrestrial ecosystem modeling of the spatial distribution of forest NEP across Japan has suggested ranges of estimates of approximately 0.5–2.0 MgC ha^{-1} yr^{-1} (Ito, 2008) and approximately 0.5–3.0 MgC ha^{-1} yr^{-1} (Sasai et al., 2011), both of which are plausible compared with the present estimate.

Remote-sensing technologies, such as synthetic aperture radar (SAR; e.g., Mermoz et al., 2015) and light detection and ranging (LiDAR; e.g., Dubayah et al., 2022), enable the measurement of forest biomass and the estimation of sequestration by detecting the change between two observation periods. Recent years have witnessed remarkable advances in SAR and LiDAR technologies, which are promising tools for estimating forest carbon stocks. However, calibration using ground-based inventory data remains indispensable, and current estimations of forest C stocks and subsequent C uptake are subject to uncertainties that limit their practical implementation (see Li et al., 2024).

Considering that eligibility for international C trading is predicated on forests treated as equivalent to those governed by the JFA, in the present study we used m-NFI_1 estimation to further quantify the time (t) variability in the total forest C stock (C_T) with changes in the total forest area (A_T) and the mean forest stand-scale C density (D), expressed as:

$$\frac{1}{C_T}\frac{dC_T}{dt} = \frac{1}{A_T}\frac{dA_T}{dt} + \frac{1}{D}\frac{dD}{dt}. \quad (4)$$

Here, Eq. (4) can be derived from the chain rule $dC_T = (\partial C_T/\partial A_T)dA_T + (\partial C_T/\partial D)dD$ where $C_T = A_T \times D$. This analysis revealed that the contributions of a decrease in forest area (the first term on the right side of Eq. (4)) and an increase in forest C density (the second term) were − 0.70% yr^{-1} and + 1.88% yr^{-1}, respectively, resulting in a growth rate of total carbon stock (the left side of Eq. (4)) of +1.18% yr^{-1}. In practice, this analysis indicates that the abandonment of reforestation following final harvesting has become common in Japan in recent years (Japan Forestry Agency, 2025), resulting in a decline in the JFA forest area. However, the biomass growth in existing forests has significantly increased the growing stock per unit area and, as a result, it has offset the reduction in JFA forest area, leading to an overall increase in the total forest growing stock in Japan.

In this study, the C sequestration capacity of *Cr. japonica* was remarkably high, with an average area-based C uptake of 3.53 MgC ha^{-1} yr^{-1} (Fig. 2a), which approaches the maximum value reported by Kondo et al. (2017). Although eddy-covariance measurements in *Cr. japonica* forests remain limited, the high value of 5.63 MgC ha^{-1} yr^{-1} observed in the southern part of Japan (Hata et al., 2023) may represent the upper tail of the NEP frequency distribution, reflecting the species' potential under optimal conditions. The combination of its highest productivity and extensive distribution across Japan enables *Cr. japonica* forests to achieve the highest total C uptake (14.9 TgC yr^{-1}; Fig. 2b), accounting for a considerable proportion of the total forest C sequestration in Japan (43.1%).

The traditional assumption that forest C uptake diminishes rapidly with maturity is increasingly viewed as outdated, as a growing body of literature demonstrates sustained productivity in older forest stands (e.g., Begović et al., 2023; Ciais et al., 2008; Luyssaert et al., 2008; Stephenson et al., 2014). Nakahata et al. (2025) showed that, for *Cr. japonica* forests across Japan, the maximum biomass accumulation and the age at which it is reached may be significantly higher than previously assumed. The present findings are consistent with this statement, in that the potential sequestration capacity for major plantation tree species remains almost constant until at least 75 years of age.

The long-standing principle integrated into Japanese forestry administrations, emphasizing the renewal of young stands based on presumed growth declines, requires urgent revision. The present results suggest that extending rotation ages could further enhance the future C sink strength of Japanese plantation forests, especially those of *Cr. japonica*.

4.2. Forest characteristics determining productivity

As previously emphasized, deriving forest C uptake by calculating the difference in forest biomass estimates from remote-sensing data, such as SAR or LiDAR data, between two time points requires an extremely long observation interval to detect significant differences, given the current uncertainties in measurement precision. Consequently, for wide-area estimation of forest C sequestration, a more pragmatic approach at present is to apply terrestrial ecosystem models calibrated with eddy-covariance data from a limited number of sites, driven by broad remotely sensed environmental data and/or reanalyzed and gridded four-dimensional meteorology datasets (see Kumagai et al., 2013). However, the eddy-covariance data required are inherently restricted to specific locations owing to installation constraints, inevitably reflecting only the average or intermediate characteristics of the region (cf. Kondo et al., 2017). Model estimates calibrated with such data tend to regress toward the mean because of statistical convergence (cf. Ito, 2008).

As a result, this approach struggles to adequately capture the dynamics of forests with exceptionally high productivity or the non-linear responses triggered by extreme meteorological events. The numerical range in national NEP estimated in the present study (Fig. 5a) is generally consistent with the model estimates by Ito (2008) and Sasai et al. (2011), and the eddy-covariance data reported by Kondo et al. (2017). Furthermore, the geographical gradient, characterized by higher NEP in the south and lower values in the north, adequately reflects the findings of these earlier studies. Nevertheless, within the framework of such wide-area estimation models, it remains difficult to capture the intense forest productivity that reaches as much as approximately 10 MgC ha^{-1} yr^{-1} recorded in field measurements (see Fig. 5a). Hata et al. (2023) reported an extremely high NEP of 5.63 (observed) to 7.52 (process-based modeled) MgC ha^{-1} yr^{-1} in situ, whereas current model estimates, including those reported in this study, have not reproduced such peaks in sequestration capacity. This implies that, while current wide-area evaluation methods are effective for showing macro-level trends, they likely continue to underestimate the potential maximum

sequestration capacity of forests and the diversity of localized environmental responses.

The magnitude of natural disturbances detected in the present study was remarkably significant and exerted a profound impact on forest C dynamics (NEP_Dist in Fig. 5b). Notably, certain forest stands exhibited C losses exceeding 20 MgC ha^{-1} yr^{-1} within the period 2009–2018. Given that forests with a carbon stock of 150 MgC ha^{-1} are broadly distributed across Japan (see Fig. 2a), these results suggest that large-scale disturbances, resulting in a 10%–20% reduction in the total C stock, are a pervasive phenomenon. In the Japanese context, the primary driver for such substantial C loss is likely the frequent impact of typhoons and related meteorological disasters (cf. Chiba, 2000; Ito, 2010; Kamimura et al., 2022). However, given that the present analysis does not account for necromass dynamics, the reported C loss may be an overestimation of immediate atmospheric emissions.

In contrast to natural disturbances, abrupt C losses attributable to forestry practices, such as harvesting, were less prominently detected (NEP_For in Fig. 5b). This reflects the predominance of clear-cutting in final harvesting in Japan, coupled with the low overall frequency of such harvesting on a national scale (cf. Japan Forestry Agency, 2025); consequently, the 4 km grid resolution of the m-NFI may fail to capture such large-scale logging operations. Ultimately, the present findings demonstrate that direct field forest inventories, such as individual tree size measurements, are capable of detecting extremes in C uptake and loss that are inherently difficult to capture using eddy-covariance observations or terrestrial ecosystem models. Accurate national accounting requires moving beyond model-based smoothing; instead, tree-level field inventories capable of capturing the extreme C uptake and loss that define real-world forest dynamics are required.

One fundamental question is raised: what are the primary determinants of the spatial distribution of forest productivity across Japan? One might intuitively assume that meteorological and environmental conditions are crucial. While these are undoubtedly the fundamental physiological drivers, our analysis revealed that forest type is the predominant determinant of productivity (Fig. 6a), followed by the initial tree size at the baseline survey, where larger trees exhibited higher subsequent growth rates (see Stephenson et al., 2014).

The relatively low SHAP values for meteorological drivers and forest age do not necessarily imply a lack of their physiological influence. Instead, in the Random Forest architecture, when several input features are statistically correlated, the model tends to attribute predictive importance to the most integrative variable, potentially overshadowing other distal drivers through a process associated with multicollinearity. In this context, forest type acts as a high-level integrative proxy that subsumes the spatial influences of climate and stand development history. This reflects a dual process: (1) intentional "site-species matching" in plantation forestry (Fujikake, 2007), where species are strategically allocated to their optimal climatic zones, and (2) natural successional processes and environmental filtering in secondary and natural forests, which align species with their suitable habitats over time. Consequently, once forest type is accounted for, the additional marginal explanatory power of individual meteorological variables becomes relatively small in the statistical model. This suggests that the observed NEP variation is not independent of climate or age, but rather reflects the integrated ecological status represented by forest type itself.

Focusing on the relative importance of specific forest types, *P. densiflora*, *L. kaempferi*, and *Abies* and *Picea* forests were the most important, but their effects on NEP (in the absence of natural disturbances and forestry practices) were negative (Fig. 6b). Given that *P. densiflora* typically occupies degraded land or dry, nutrient-poor ridges, and L. *kaempferi* or *Abies* and *Picea* are found in subalpine or colder regions, the reduction in regional NEP is ecologically consistent (see Numata and Iwase, 2002). Conversely, *Quercus* unexpectedly had the strongest positive effect to increase NEP. Given that this analysis excluded the impacts of natural disturbances and forestry practices, these results imply that, in terms of latent biological potential, *Quercus* may show the highest productivity in Japan, surpassing unmanaged major coniferous plantations. However, Japanese oak wilt is currently a serious disease in Japan (cf. Imamura et al., 2017), hence excluding its impact from the present analysis may have further elevated the estimated NEP of *Quercus*. When properly managed, the productivity of *Cr. japonica* and *Ch. obtusa* plantations can be greatly enhanced (Fig. 2a). This underscores the profound influence of anthropogenic forest management in maximizing the C sequestration capacity of Japan's forest ecosystems.

5. Conclusions

Japan aims to achieve C neutrality by 2050. Currently, government projections estimate annual forest C uptake at approximately 50 million tons of CO_2, predicting a decline to 40 million tons of CO_2 reflecting the aging of forest stands (Center for Research and Development Strategy, 2022). The present study, based on rigorous empirical evidence, reveals a starkly different reality: current annual forest C uptake is approximately 169 million tons of CO_2, and is as high as 127 million tons of CO_2 when considering only JFA-governed forests. These figures necessitate a substantial upward revision of the conventional official estimates provided by the Japan Forestry Agency. Furthermore, the findings suggest that this robust C sequestration capacity is unlikely to diminish in the foreseeable future.

Our previous research (Egusa et al., 2024) demonstrated that C storage can be dramatically enhanced by revitalizing forestry, increasing timber production, and ensuring the long-term storage of C in wood products. Ultimately, the findings correct the previous underestimations in official reports and presentations, thereby revealing the true magnitude of C sequestration in Japan's forests. We hope that these findings will be actively utilized to inform environmental policies and forest management strategies, ensuring that the full potential of Japan's forests in achieving C neutrality is realized.

CRediT authorship contribution statement

Tomo'omi Kumagai: Writing – review & editing, Writing – original draft, Project administration, Methodology, Funding acquisition, Formal analysis, Data curation, Conceptualization. **Ryo Nakahata:** Writing – review & editing, Formal analysis, Data curation. **Toshiaki Kameyama:** Writing – review & editing, Formal analysis, Data curation. **Tomohiro Egusa:** Writing – review & editing, Formal analysis, Data curation.

Funding sources

The funding for this work was supported by the Kanagawa Prefectural Government, Japan, as part of the project on "Forest, soil, and water resource conservation in the western Kanagawa reservoir area"; and by Grants-in-Aid for Scientific Research (grant number 21H05316) from the Ministry of Education, Culture, Sports, Science and Technology, Japan.

Declaration of competing interest

The authors declare that they have no known competing financial interests or personal relationships that could have appeared to influence the work reported in this paper.

Acknowledgments

This study was supported in part by the findings from Takafumi Tabuchi's undergraduate thesis, supervised by T. K. at The University of Tokyo. We thank Robert McKenzie from Edanz (https://jp.edanz.com/ac) for editing the English text of a draft of this manuscript.

Appendix

To ensure model reproducibility and eliminate potential overfitting bias in ecological interpretation, the original dataset ($N = 7043$) was randomly partitioned into a training and validation set (80%, $n = 5634$) and an independent test set (20%, $n = 1409$). Hyperparameter tuning was performed exclusively within the training set using Bayesian optimization to minimize the five-fold cross-validation MSE over 5000 iterations. Table A1 summarizes the partitioning details, the search space for each hyperparameter, and the final configurations used in the predictive model.

Appendix Table A1
Data partitioning, hyperparameter search space, and Bayesian optimization settings for the random forest model.

Category	Item	Description/setting
Data partitioning	Training vs. Independent test	8: 2 ($n = 5634$, 1409)
Optimization strategy	Algorithm	Bayesian optimization
	Objective function	5-fold cross-validation MSE (within training set)
	Iterations	5000 objective function evaluations
Hyperparameters	Number of trees	[10, 5000]
	Max number of splits	[1, 2252]
	Min leaf size	[1, 4507]
	Predictor selection	[1, 7]
Split criterion	Interaction test	To ensure unbiased selection for categorical features

For the Random Forest (RF) model, performance metrics are reported as the mean values across the five test folds to ensure generalizability. The Generalized Linear Model (GLM) was similarly evaluated using the mean performance across the test folds to provide a consistent linear baseline.

Appendix Table A2
Predictive performance metrics (R^2, RMSE, and MAE) for the RF model and the GLM used as a baseline for Fig. 6a.

Model	Evaluation dataset	R^2	RMSE	MAE
RF	Test (5-fold CV mean)	0.147	2.605	2.050
	Training and validation set	0.240	2.467	1.941
GLM (Baseline)	Test (5-fold CV mean)	0.123	2.642	2.067

A SHAP dependency plot indicates how a single input parameter affects the output of the machine-learning model. To ensure the generalizability of the model interpretation, SHAP values were calculated exclusively for the independent test set (n = 1409), which was not used during model training or optimization. The SHAP values for specific input features, such as forest age and forest type ID, increase as positive/negative values, representing an increase/decrease in net ecosystem productivity (Fig. A1). Fig. 6a and b were generated by averaging all absolute SHAP values for each input parameter and averaging SHAP values for each forest type ID, respectively.

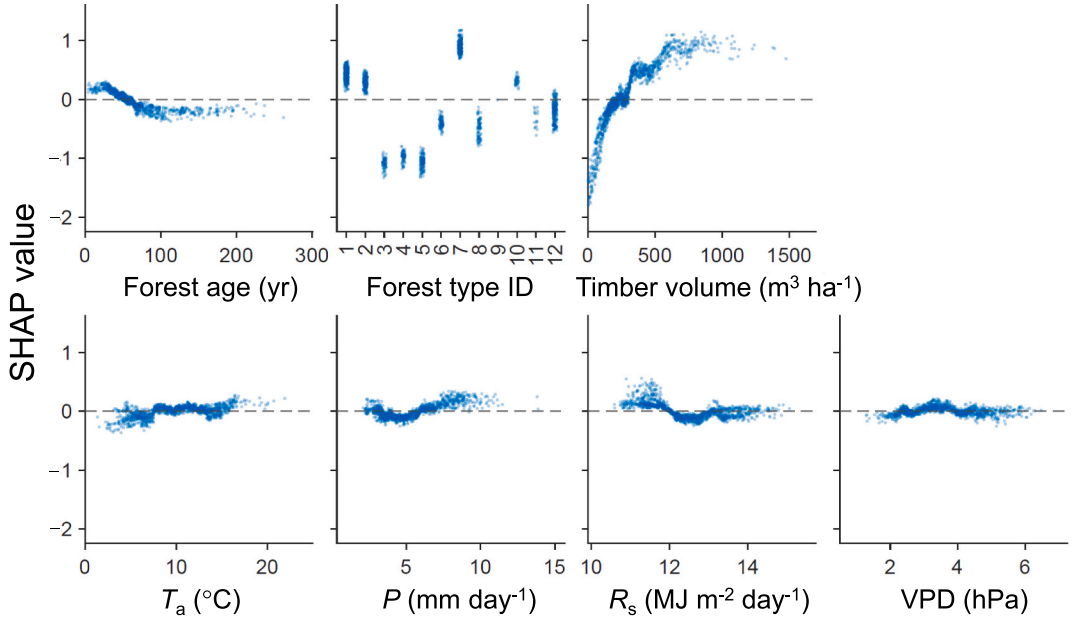

Appendix Fig. A1. Shapley additive explanation (SHAP) dependency plot for each forest characteristic and meteorological driver in Fig. 6a. To ensure the objectivity of the ecological interpretation and avoid overfitting bias, all SHAP values were calculated exclusively using the independent test set ($n = 1409$). Forest type ID: 1, *Cryptomeria japonica*; 2, *Chamaecyparis obtusa*; 3, *Pinus densiflora*; 4, *Larix kaempferi*; 5, *Abies* and *Picea*; 6, *Fagus*; 7, *Quercus*; 8, Betulaceae; 9, Coniferous and broad-leaved mixed forests; 10, Evergreen broad-leaved forests; 11, Other coniferous forests; 12, Other broad-leaved forests. Note that "Coniferous and broad-leaved mixed forests" (ID 9) is not shown in Fig. 6b due to an insufficient number of SHAP values.

Data availability

Data will be made available on request.

References

Begović, K., Schurman, J.S., Svitok, M., Pavlin, J., Langbehn, T., Svobodová, K., Mikoláš, M., Janda, P., Synek, M., Marchand, W., 2023. Large old trees increase growth under shifting climatic constraints: aligning tree longevity and individual growth dynamics in primary mountain spruce forests. Glob. Chang. Biol. 29, 143–164.

Birdsey, R.A., Plantinga, A.J., Heath, L.S., 1993. Past and prospective carbon storage in United States forests. For. Ecol. Manag. 58, 33–40.

Booth, B.B., Jones, C.D., Collins, M., Totterdell, I.J., Cox, P.M., Sitch, S., Huntingford, C., Betts, R.A., Harris, G.R., Lloyd, J., 2012. High sensitivity of future global warming to land carbon cycle processes. Environ. Res. Lett. 7, 024002.

Breiman, L., 2001. Random forests. Mach. Learn. 45, 5–32.

Center for Research and Development Strategy, 2022. Research Report: Negative Emission Technologies Using Biomass as a CO_2 Sink (CRDS-FY2021-RR-05). Japan Science and Technology Agency, Tokyo (in Japanese). Available at https://www.jst.go.jp/crds/pdf/2021/RR/CRDS-FY2021-RR-05.pdf (accessed 1 April 2026).

Chiba, Y., 2000. Modelling stem breakage caused by typhoons in plantation *Cryptomeria japonica* forests. For. Ecol. Manag. 135, 123–131.

Ciais, P., Schelhaas, M.-J., Zaehle, S., Piao, S.L., Cescatti, A., Liski, J., Luyssaert, S., Le-Maire, G., Schulze, E.-D., Bouriaud, O., 2008. Carbon accumulation in European forests. Nat. Geosci. 1, 425–429.

Dubayah, R., Armston, J., Healey, S.P., Bruening, J.M., Patterson, P.L., Kellner, J.R., Duncanson, L., Saarela, S., Ståhl, G., Yang, Z., 2022. GEDI launches a new era of biomass inference from space. Environ. Res. Lett. 17, 095001.

Eggers, J., Lindner, M., Zudin, S., Zaehle, S., Liski, J., 2008. Impact of changing wood demand, climate and land use on European forest resources and carbon stocks during the 21st century. Glob. Chang. Biol. 14, 2288–2303.

Egusa, T., Kumagai, T., Shiraishi, N., 2020. Carbon stock in Japanese forests has been greatly underestimated. Sci. Rep. 10, 7895.

Egusa, T., Nakahata, R., Neumann, M., Kumagai, T., 2024. Carbon stock projection for four major forest plantation species in Japan. Sci. Total Environ. 927, 172241.

Fang, J., Chen, A., Peng, C., Zhao, S., Ci, L., 2001. Changes in forest biomass carbon storage in China between 1949 and 1998. Science 292, 2320–2322.

Fang, J., Oikawa, T., Kato, T., Mo, W., Wang, Z., 2005. Biomass carbon accumulation by Japan's forests from 1947 to 1995. Glob. Biogeochem. Cycles 19.

Fujikake, I., 2007. Selection of tree species for plantations in Japan. Forest Policy Econ. 9, 811–821.

Hata, Y., Kumagai, T., Shimizu, T., Miyazawa, Y., 2023. Implications of seasonal changes in photosynthetic traits and leaf area index for canopy CO_2 and H_2O fluxes in a Japanese cedar (*Cryptomeria japonica* D. Don) plantation. Ecol. Model. 477, 110271.

Hilker, T., Coops, N.C., Wulder, M.A., Black, T.A., Guy, R.D., 2008. The use of remote sensing in light use efficiency based models of gross primary production: a review of current status and future requirements. Sci. Total Environ. 404, 411–423.

Hosoda, K., Mitsuda, Y., Iehara, T., 2010. Differences between the present stem volume tables and the values of the volume equations, and their correction. Jpn. J. For. Plan. 44, 23–39 (in Japanese with English abstract).

Hu, H., Wang, S., Guo, Z., Xu, B., Fang, J., 2015. The stage-classified matrix models project a significant increase in biomass carbon stocks in China's forests between 2005 and 2050. Sci. Rep. 5, 11203.

Imamura, K., Managi, S., Saito, S., Nakashizuka, T., 2017. Abandoned forest ecosystem: implications for Japan's oak wilt disease. J. Forest Econ. 29, 56–61.

Ito, A., 2008. The regional carbon budget of East Asia simulated with a terrestrial ecosystem model and validated using AsiaFlux data. Agric. For. Meteorol. 148, 738–747.

Ito, A., 2010. Evaluation of the impacts of defoliation by tropical cyclones on a Japanese forest's carbon budget using flux data and a process-based model. J. Geophys. Res. Biogeosci. 115.

Japan Forestry Agency, 1970a. Tables for calculating stem volume from diameter at breast height and tree height in eastern Japan. Japan Forestry Agency, Tokyo (in Japanese). [Official volume tables widely used for National Forest Inventories in Japan].

Japan Forestry Agency, 1970b. Tables for calculating stem volume from diameter at breast height and tree height in western Japan. Japan Forestry Agency, Tokyo (in Japanese). [Official volume tables widely used for National Forest Inventories in Japan].

Japan Forestry Agency, 2015. Report of the accuracy verification survey for the 4th period forest ecosystem diversity survey in 2014. Japan Forestry Agency, Tokyo (in Japanese). [Official technical report for the National Forest Inventory in Japan].

Japan Forestry Agency, 2019. Report of the accuracy verification survey for the 4th period forest ecosystem diversity survey in 2018. Japan Forestry Agency, Tokyo (in Japanese). [Official technical report for the National Forest Inventory in Japan].

Japan Forestry Agency, 2025. Annual Report on Forest and Forestry in Japan, Fiscal Year 2024. Ministry of Agriculture, Forestry and Fisheries, Japan, Tokyo (in Japanese with English abstract).

Kamimura, K., Nanko, K., Matsumoto, A., Ueno, S., Gardiner, J., Gardiner, B., 2022. Tree dynamic response and survival in a category-5 tropical cyclone: the case of super typhoon Trami. Sci. Adv. 8, eabm7891.

Kauppi, P.E., Mielikäinen, K., Kuusela, K., 1992. Biomass and carbon budget of European forests, 1971 to 1990. Science 256, 70–74.

Kauppi, P.E., Rautiainen, A., Korhonen, K.T., Lehtonen, A., Liski, J., Nöjd, P., Tuominen, S., Haakana, M., Virtanen, T., 2010. Changing stock of biomass carbon in a boreal forest over 93 years. For. Ecol. Manag. 259, 1239–1244.

Kitahara, F., Mizoue, N., Yoshida, S., 2009. Evaluation of data quality in Japanese national forest inventory. Environ. Monit. Assess. 159, 331–340.

Kondo, M., Saitoh, T.M., Sato, H., Ichii, K., 2017. Comprehensive synthesis of spatial variability in carbon flux across monsoon Asian forests. Agric. For. Meteorol. 232, 623–634.

Kumagai, T., Kanamori, H., Yasunari, T., 2013. Deforestation-induced reduction in rainfall. Hydrol. Process. 27, 3811–3814.

Li, H., Hiroshima, T., Li, X., Hayashi, M., Kato, T., 2024. High-resolution mapping of forest structure and carbon stock using multi-source remote sensing data in Japan. Remote Sens. Environ. 312, 114322.

Lundberg, S.M., Lee, S.-I., 2017. A unified approach to interpreting model predictions. Adv. Neural Inf. Proces. Syst. 30.

Luyssaert, S., Schulze, E.-D., Börner, A., Knohl, A., Hessenmöller, D., Law, B.E., Ciais, P., Grace, J., 2008. Old-growth forests as global carbon sinks. Nature 455, 213–215.

Mermoz, S., Réjou-Méchain, M., Villard, L., Le Toan, T., Rossi, V., Gourlet-Fleury, S., 2015. Decrease of L-band SAR backscatter with biomass of dense forests. Remote Sens. Environ. 159, 307–317.

Nakahata, R., Egusa, T., Kumagai, T., 2025. Current and future carbon stocks of a dominant forest plantation species, *Cryptomeria japonica*, throughout Japan. J. Environ. Manag. 393, 126981.

Norishige, R., Ota, T., Furuta, M., Mizoue, N., Hosaka, T., 2025. Reforestation and natural regeneration status of non-reforestation land on Kyushu Island. J. Jpn. For. Soc. 107, 135–142 (in Japanese with English abstract).

Numata, M., Iwase, T., 2002. Vegetation of Japan, Illustrated. Kodansha Ltd., Tokyo (in Japanese). ISBN: 9784061595347).

Pan, Y., Birdsey, R.A., Fang, J., Houghton, R., Kauppi, P.E., Kurz, W.A., Phillips, O.L., Shvidenko, A., Lewis, S.L., Canadell, J.G., 2011. A large and persistent carbon sink in the world's forests. Science 333, 988–993.

Pan, Y., Birdsey, R.A., Phillips, O.L., Houghton, R.A., Fang, J., Kauppi, P.E., Keith, H., Kurz, W.A., Ito, A., Lewis, S.L., 2024. The enduring world forest carbon sink. Nature 631, 563–569.

Pei, Y., Dong, J., Zhang, Y., Yuan, W., Doughty, R., Yang, J., Zhou, D., Zhang, L., Xiao, X., 2022. Evolution of light use efficiency models: improvement, uncertainties, and implications. Agric. For. Meteorol. 317, 108905.

Sasai, T., Saigusa, N., Nasahara, K.N., Ito, A., Hashimoto, H., Nemani, R., Hirata, R., Ichii, K., Takagi, K., Saitoh, T.M., 2011. Satellite-driven estimation of terrestrial carbon flux over Far East Asia with 1-km grid resolution. Remote Sens. Environ. 115, 1758–1771.

Stephenson, N.L., Das, A.J., Condit, R., Russo, S.E., Baker, P.J., Beckman, N.G., Coomes, D.A., Lines, E.R., Morris, W.K., Rüger, N., 2014. Rate of tree carbon accumulation increases continuously with tree size. Nature 507, 90–93.

Takamura, N., Hata, Y., Matsumoto, K., Kume, T., Ueyama, M., Kumagai, T., 2023. El Niño-Southern Oscillation forcing on carbon and water cycling in a Bornean tropical rainforest. Proc. Natl. Acad. Sci. 120, e2301596120.

UNFCCC, 2002. Report of the conference of the parties on its seventh session, held at Marrakesh from 29 October to 10 November 2001. Addendum. Part two: Action taken by the Conference of the Parties. Volume I.

UNFCCC, 2019. Report of the Conference of the Parties serving as the meeting of the Parties to the Paris Agreement on the third part of its first session, held in Katowice from 2 to 15 December 2018. Addendum 1. Part two: Action taken by the Conference of the Parties serving as the meeting of the Parties to the Paris Agreement.

Wear, D.N., Coulston, J.W., 2015. From sink to source: regional variation in US forest carbon futures. Sci. Rep. 5, 16518.